Application of SVC for Electromechanical Oscillation Damping Improvement in Multi-Machine Power System

RUDY GIANTO
Department of Electrical Engineering
University of Tanjungpura
Jalan Prof. Dr. H. Hadari Nawawi Pontianak 78124
INDONESIA
rudygianto@gmail.com

Abstract: - SVC (Static Var Compensator) is the most popular and widely used FACTS (Flexible AC Transmission System) device. This device has the ability to provide dynamic shunt compensation, and therefore, it is usually used for continuously regulating power flow and voltage stabilization. However, by adding a suitable supplementary controller, the device can also be used for system electromechanical oscillation damping improvement. The research reported in this paper investigates the application of SVC in improving system oscillation damping and stability of interconnected multi-machine electric power system. Verification using eigenvalues analysis and time-domain simulations confirm the capability of the device in providing better system damping and stability.

Key-Words: SVC, PSS, damping, electromechanical oscillation, power system

1 Introduction

For secure power system operation, one important factor that should be considered is the system stability. It has been known that the system stability, particularly small-disturbance stability, is closely related to the damping of system electromechanical oscillation where a good damping implies a good system dynamic performance and stability.

The application of PSS and FACTS devices in electromechanical oscillation damping improvement has also been widely acknowledged. Although the main purpose of FACTS device is for controlling system voltage and power flow, by employing a suitable supplementary controller, the device can be used for damping improvement tool.

Among the various FACTS devices, SVC is the most popular and widely used FACTS device. It is the first FACTS device and was brought to market by Electric Power Research Institute (EPRI) approximately two decades ago. At the present, more than 800 SVCs have been installed worldwide and used mainly for voltage stabilization and reactive-power compensation [1].

An SVC consists of a fast thyristor switch controlling a shunt capacitor bank and/or a reactor, to provide dynamic shunt compensation. This dynamic shunt compensation continuously adjusts the reactive-power output and thus maintaining the voltage at required level. The SVC capability in controlling transmittable power also implies the potential application of the device for the enhancement of system dynamic performance.

The application of SVC and its control co-ordination with PSSs for power system stability improvement has been investigated by several researchers [2-6]. In the investigation [2, 3], SVC was used to enhance the stability of a small power system (i.e. single machine system). In [4-6], the coordinated design problem of PSSs and SVC was handled as an optimization problem, where particle swarm [4, 5] and grey wolf [6] optimizers have been used to solve the optimization problem. The design strategy has been used to improve the stability of multi-machine power systems.

In [7, 8], a general design procedure has been proposed for optimal control co-ordination amongst PSSs and FACTS devices. The method has been applied to power systems installed with TCSC (Thyristor Controlled Series Capacitor) and UPFC (Unified Power Flow Controller). Therefore, against the above background, the objective of the present paper is to apply and extend the investigation in [7, 8] to multi-machine power system installed with SVC. Specifically, the main contributions of the present paper can be described as follows: (i) development of general mathematical model of multi-SVC in multi-machine power system environment for stability studies. By using the mathematical formulation proposed, any number of SVCs (installed in any buses) can be modelled

without difficulty. Also it can be applied to any size of power system; (ii) application and extension of the method for control coordination of PSSs and SVC proposed in [2] to multi-machine power system, with a particular reference to the enhancement of inter-area mode damping. The performance of FACTS device (i.e. SVC) in improving system stability and dynamic performance is validated by eigenvalues analysis and time-domain simulations of the power system.

2 SVC Dynamic Model

In Figure 1 is shown in a block diagram form the control system of an SVC [9, 10] used in the present work. In Figure 1, B_c represents SVC susceptance and V_T is the terminal voltage where the SVC is installed. For stability improvement purpose, a supplementary signal (X_{SDC}) derived from a separate controller is input to the main controller as shown in Figure 1. The state equations for the SVC main control system can be arranged as follows:

$$\dot{\boldsymbol{x}}_S = \boldsymbol{A}_S \boldsymbol{x}_S + \boldsymbol{C}_S |V_T| + \boldsymbol{B}_S X_{SDC} + \boldsymbol{D}_S V_T^{ref} \qquad (1)$$

where $\boldsymbol{x}_S$ is the state vector for the SVC main control system; $\boldsymbol{A}_s$, $\boldsymbol{B}_s$, $\boldsymbol{C}_s$, and $\boldsymbol{D}_s$ are matrices the elements of which depend on the gains and time constants of the controllers. Expressions for these matrices can be found in Appendix A.1.

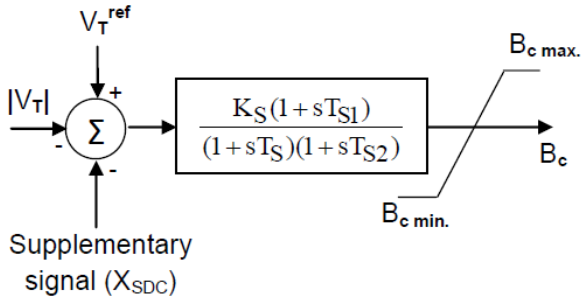

Figure 1 Control block diagram of SVC

Dynamic performance improvement with FACTS devices is effected through power modulation by a supplementary controller. Figure 2 shows the control block diagram used in the present work [1, 7, 8]. The state equation for the supplementary controller can be written in compact form as follows:

$$\dot{\boldsymbol{x}}_{su} = \boldsymbol{A}_{su} \boldsymbol{x}_{su} + \boldsymbol{C}_{su} \dot{P}_T \qquad (2)$$

where $\boldsymbol{x}_{su}$ is the vector of state variables of the supplementary controller; $\boldsymbol{A}_{su}$ and $\boldsymbol{C}_{su}$ are matrices the elements of which depend on the gains and time constants of the controller. Expressions for these matrices can also be found in Appendix A.1

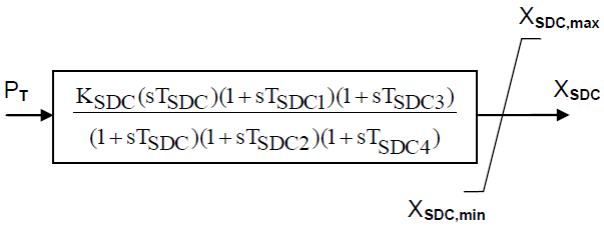

Figure 2 Supplementary control block diagram

3 Multi-Machine System Model

3.1 Power System Network Model

Figure 3 shows an NB-node power system considered in this paper. It is to be assumed that NG generators are connected to the power system. The network nodal current vector $\boldsymbol{I}$ and nodal voltage vector $\boldsymbol{V}$ for the system are related by:

$$\boldsymbol{I} = \boldsymbol{Y}\boldsymbol{V} \qquad (3)$$

where $\boldsymbol{Y}$ is the system admittance matrix.

All of the quantities in (3) are, in general, complex numbers. Separating (3) into real and imaginary parts and rearranging, leads to the following equation where all of the vector/matrix coefficients are real:

$$\boldsymbol{I}_N = \boldsymbol{Y}_N \boldsymbol{V}_N \qquad (4)$$

where:

$$\boldsymbol{I}_N = \begin{bmatrix} re(I_1) \\ im(I_1) \\ \cdots\cdots \\ re(I_2) \\ im(I_2) \\ \cdots\cdots \\ \vdots \\ \cdots\cdots \\ re(I_{NB}) \\ im(I_{NB}) \end{bmatrix}; \boldsymbol{V}_N = \begin{bmatrix} re(V_1) \\ im(V_1) \\ \cdots\cdots \\ re(V_2) \\ im(V_2) \\ \cdots\cdots \\ \vdots \\ \cdots\cdots \\ re(V_{NB}) \\ im(V_{NB}) \end{bmatrix} \qquad (5)$$

and:

$$\boldsymbol{Y}_N = \begin{bmatrix} re(Y_{11}) & -im(Y_{11}) & \vdots & re(Y_{12}) & -im(Y_{12}) & \vdots & \cdots & \vdots & re(Y_{1,NB}) & -im(Y_{1,NB}) \\ im(Y_{11}) & re(Y_{11}) & \vdots & im(Y_{12}) & re(Y_{12}) & \vdots & \cdots & \vdots & im(Y_{1,NB}) & re(Y_{1,NB}) \\ \cdots\cdots & \cdots\cdots & \vdots & \cdots\cdots & \cdots\cdots & \vdots & \cdots & \vdots & \cdots\cdots & \cdots\cdots \\ re(Y_{21}) & -im(Y_{21}) & \vdots & re(Y_{22}) & -im(Y_{22}) & \vdots & \cdots & \vdots & re(Y_{2,NB}) & -im(Y_{2,NB}) \\ im(Y_{21}) & re(Y_{21}) & \vdots & im(Y_{22}) & re(Y_{22}) & \vdots & \cdots & \vdots & im(Y_{2,NB}) & re(Y_{2,NB}) \\ \cdots\cdots & \cdots\cdots & \vdots & \cdots\cdots & \cdots\cdots & \vdots & \cdots & \vdots & \cdots\cdots & \cdots\cdots \\ \vdots & \vdots & \vdots & \vdots & \vdots & \vdots & \ddots & \vdots & \vdots & \vdots \\ \cdots\cdots & \cdots\cdots & \vdots & \cdots\cdots & \cdots\cdots & \vdots & \cdots & \vdots & \cdots\cdots & \cdots\cdots \\ re(Y_{NB,1}) & -im(Y_{NB,1}) & \vdots & re(Y_{NB,2}) & -im(Y_{NB,2}) & \vdots & \cdots & \vdots & re(Y_{NB,NB}) & -im(Y_{NB,NB}) \\ im(Y_{NB,1}) & re(Y_{NB,1}) & \vdots & im(Y_{NB,2}) & re(Y_{NB,2}) & \vdots & \cdots & \vdots & im(Y_{NB,NB}) & re(Y_{NB,NB}) \end{bmatrix} \quad (6)$$

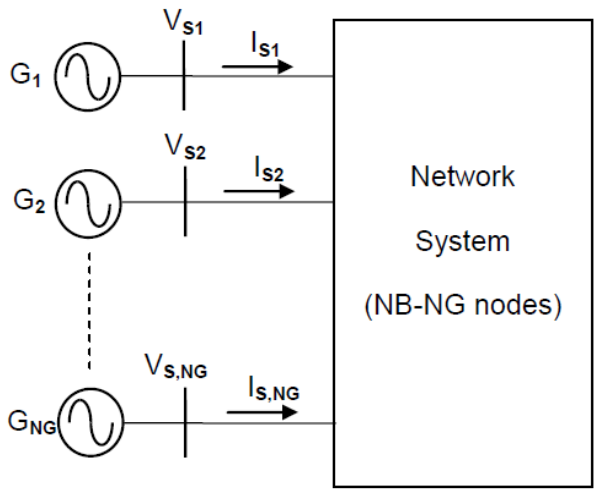

Figure 3 Multi-machine power system

In (3), the static loads of constant admittance form and fixed form of reactive power compensation are included in the system admittance matrix. In this way, the nodal currents in vector $\boldsymbol{I}$ are non-zero only at generator nodes. Therefore, (3) can be partitioned as follows:

$$\begin{bmatrix} \boldsymbol{I}_{SN} \\ \cdots\cdots \\ \boldsymbol{I}_{LN} = \boldsymbol{0} \end{bmatrix} = \begin{bmatrix} \boldsymbol{Y}_{SS} & \vdots & \boldsymbol{Y}_{SL} \\ \cdots\cdots & \cdots & \cdots\cdots \\ \boldsymbol{Y}_{LS} & \vdots & \boldsymbol{Y}_{LL} \end{bmatrix} \begin{bmatrix} \boldsymbol{V}_{SN} \\ \cdots\cdots \\ \boldsymbol{V}_{LN} \end{bmatrix} \quad (7)$$

where:
S: set of generator nodes
L: set of non-generator nodes
$\boldsymbol{I}_{SN}$, $\boldsymbol{V}_{SN}$: vectors of network nodal currents and voltages at generator nodes respectively
$\boldsymbol{V}_{LN}$: vector of nodal voltages at the remaining nodes in the system
$\boldsymbol{Y}_{SS}$, $\boldsymbol{Y}_{SL}$, $\boldsymbol{Y}_{LS}$ and $\boldsymbol{Y}_{LL}$: submatrices from partitioning of $\boldsymbol{Y}$ matrix

Based on (7), the following equations are obtained:

$$\boldsymbol{I}_{SN} = \boldsymbol{Y}_{SS}\boldsymbol{V}_{SN} + \boldsymbol{Y}_{SL}\boldsymbol{V}_{LN} \quad (8)$$

$$\boldsymbol{0} = \boldsymbol{Y}_{LS}\boldsymbol{V}_{SN} + \boldsymbol{Y}_{LL}\boldsymbol{V}_{LN} \quad (9)$$

It can be seen that the network model for multi-machine power system is described by two sets of algebraic equations (8) and (9). It is also to be noted that the algebraic (non-state) variables of the network model of the system are $\boldsymbol{V}_{sN}$, $\boldsymbol{I}_{sN}$ and $\boldsymbol{V}_{LN}$.

3.2 Network Model for System with SVC

Figure 4 shows a multi-machine power system installed with SVCs. In order to illustrate the mathematical formulation for modelling the power system network, it is to be assumed that the SVCs are installed as shown in Figure 4. In Figure 4, NS is the number of SVCs.

In partitioned form, the network model for the multi-machine power system installed with SVCs can be described by:

$$\begin{bmatrix} \boldsymbol{I}_{SN} \\ \cdots\cdots \\ \boldsymbol{I}_{LN} = \boldsymbol{0} \end{bmatrix} = \begin{bmatrix} \boldsymbol{Y}_{SS} & \vdots & \boldsymbol{Y}_{SL} \\ \cdots\cdots & \cdots & \cdots\cdots \\ \boldsymbol{Y}_{LS} & \vdots & \boldsymbol{Y}_{LL} + \boldsymbol{Y}_{FS} \end{bmatrix} \begin{bmatrix} \boldsymbol{V}_{SN} \\ \cdots\cdots \\ \boldsymbol{V}_{LN} \end{bmatrix} \quad (10)$$

The submatrix $\boldsymbol{Y}_{FS}$ in (10) has the same dimension as submatrix $\boldsymbol{Y}_{LL}$ and is given by:

$$Y_{FS} = \begin{array}{c} \begin{matrix} L_{NG+} & & L_{x1} & & L_{x2} & & L_{NB} \end{matrix} \\ \begin{bmatrix} \vdots & \vdots & \vdots & \vdots & \vdots & \vdots & \vdots \\ \cdots & \cdots & \cdots & \cdots & \cdots & \cdots & \cdots \\ \vdots & \vdots & \vdots & \vdots & \vdots & \vdots & \vdots \\ \cdots & \cdots & \cdots & -B_{C1} & \cdots & \cdots & \cdots \\ \vdots & \vdots & \vdots & \vdots & \vdots & \vdots & \vdots \\ \cdots & \cdots & \cdots & B_{C1} & \cdots & \cdots & \cdots \\ \vdots & \vdots & \vdots & \vdots & \vdots & \vdots & \vdots \\ \cdots & \cdots & \cdots & \cdots & \cdots & -B_{C2} & \cdots \\ \vdots & \vdots & \vdots & \vdots & \vdots & \vdots & \vdots \\ \cdots & \cdots & \cdots & \cdots & B_{C2} & \cdots & \cdots \\ \vdots & \vdots & \vdots & \vdots & \vdots & \vdots & \vdots \end{bmatrix} \end{array} \begin{array}{l} L_{NG+1} \\ \\ L_{x1} \\ \\ L_{x2} \\ \\ L_{NB} \end{array} \tag{11}$$

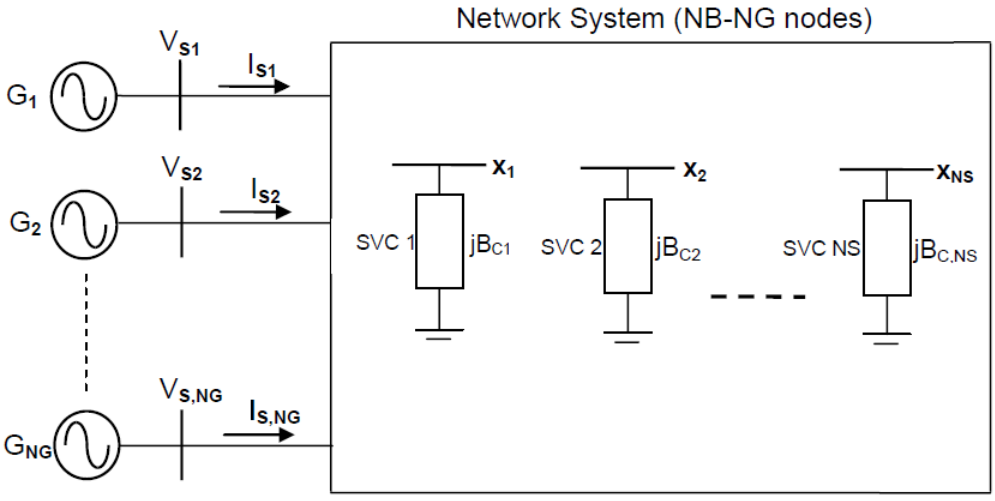

Figure 4 Multi-machine power system with SVCs

Based on (10), the following equation is obtained:

$$\mathbf{0} = \mathbf{Y}_{LS}\mathbf{V}_{SN} + (\mathbf{Y}_{LL} + \mathbf{Y}_{FS})\mathbf{V}_{LN} \quad (11)$$

The above discussion shows that the network model for multi-machine power system installed with SVCs can be described by two sets of algebraic equations (8) and (11). It is also to be noted that the algebraic (non-state) variables of the network model of the system are $\mathbf{V}_{sN}$, $\mathbf{I}_{sN}$ and $\mathbf{V}_{LN}$.

3.3 Complete System Dynamic Model

Sections 3.1 and 3.2 show that the dynamic model of power system network installed with SVC is of the form of nonlinear differential-algebraic equations (DAEs). The set of DAEs is then combined with the dynamic model of synchronous generators and other rotating machines (including their controllers) in the power system. It can be shown that the combined set of equations can be written in a compact form as follows:

$$\begin{aligned} \dot{\mathbf{x}} &= \mathbf{f}(\mathbf{x},\mathbf{w}) \\ \mathbf{0} &= \mathbf{g}(\mathbf{x},\mathbf{w}) \end{aligned} \quad (12)$$

where: $\mathbf{x}$ is the vector of state variables; $\mathbf{w}$ is the vector of non-state (algebraic) variables; $\mathbf{f}$ and $\mathbf{g}$ are nonlinear vector functions the individual expressions of which have been given in the previous sections.

The small-disturbance model of the power system installed with SVC is obtained by linearising the differential-algebraic equations which can also be written in a more compact form as follows:

$$\begin{pmatrix} \Delta\dot{\mathbf{x}} \\ \mathbf{0} \end{pmatrix} = \begin{pmatrix} \mathbf{J}_1 & \mathbf{J}_2 \\ \mathbf{J}_3 & \mathbf{J}_4 \end{pmatrix} \begin{pmatrix} \Delta\mathbf{x} \\ \Delta\mathbf{w} \end{pmatrix} \quad (13)$$

where $\mathbf{J}_1$, $\mathbf{J}_2$, $\mathbf{J}_3$, and $\mathbf{J}_4$ are matrices the elements of which are defined based on the power system initial operating condition and the parameters of the system together with its controllers. By reducing (13), the following equation is obtained:

$$\Delta\dot{\mathbf{x}} = \mathbf{A}\Delta\mathbf{x} \quad (14)$$

where $\mathbf{A} = \mathbf{J}_1 - \mathbf{J}_2\mathbf{J}_4^{-1}\mathbf{J}_3$ is the system state matrix needed for evaluation the dynamic characteristic of the power system. The state matrix is the function of controllers (PSSs and SVC devices together with their supplementary controllers) parameters.

4 Results and Discussion

4.1 Test System

The power system used in the investigation is the two-area system shown in Figure 5 [11]. It is a 4 generator, 12 bus system with a total connected load of 2734 MW. The two areas are connected by two transmission lines (two tie lines). Data for this test system is presented in Appendix A.2. For the 4-machine system, the number of electromechanical modes of oscillations will be three (two local modes and one inter-area mode). As there is a strong connection between inter-area mode of oscillation and system dynamic performance, the inter-area mode will be the focus of the investigation.

In Table 1 are given the values of electromechanical inter-area mode eigenvalue, frequency, and damping ratio for the system of Figure 5. As can be seen from Table 1, the damping ratio of the inter-area mode is low which indicates poor system dynamic performance. Stabilization measure is, then, required for improving the damping of the inter-area oscillation.

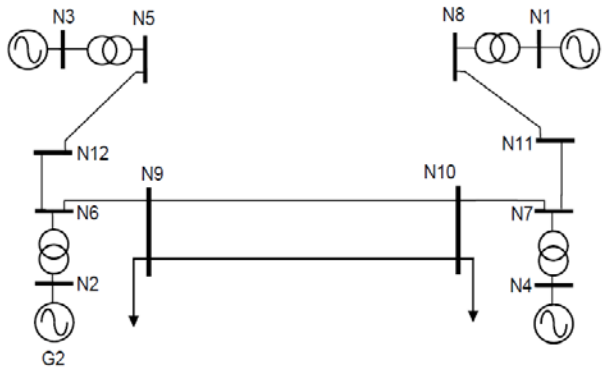

Figure 5 Two-area system

Table 1 Electromechanical inter-area mode for system of Figure 5

Eigenvalue	Frequency (Hz)	Damping Ratio
-0.3224±j4.3391	0.69	0.0741

Therefore, in order to improve the dynamic performance, it is proposed to install two PSSs in the system (in generators G1 and G3). The locations of the PSSs were determined using participation factor technique. In Table 2 are given the values of electromechanical inter-area mode eigenvalue, frequency, and damping ratio for the system with PSSs. It is to be noted that optimal values of PSSs parameters were used in the investigation. These values are given in Table 3 and were obtained using the method proposed in [7, 8].

It can be seen from Table 2 that damping ratio of the inter-area mode is 0.1442. Although it has been considered in [12, 13] that the damping ratio greater than 0.1 is acceptable; however, as mentioned in [14, 15], a minimum damping ratio of 0.15 is desirable for ensuring faster settling time of the oscillations.

Table 2 Electromechanical inter-area mode for system with PSSs

Eigenvalue	Frequency (Hz)	Damping Ratio
-0.6103±j4.1885	0.67	0.1442

Table 3 PSSs parameters

Parameter	PSS at G1	PSS at G3
K_{PSS}	14.1075 pu	15.8603 pu
T_{PSS}	1.0000 s	1.0125 s
T_{PSS1}	0.3329 s	0.3463 s
T_{PSS2}	0.3489 s	0.0796 s
T_{PSS3}	0.2160 s	0.1355 s
T_{PSS4}	0.0795 s	0.3177 s

4.2 Application of SVC

In order to ensure faster settling time, it is proposed to further improve system dynamic performance by installing a supplementary control in the SVC in node N10. The SVC has been installed for the primary purpose of voltage stabilization and reactive-power compensation. An opportunity is then taken to equip the SVC installed with a supplementary control to provide a secondary function for damping improvement of the electromechanical modes, particularly the inter-area mode.

In Table 4 are given the values of electromechanical mode eigenvalue, frequency, and damping ratio for the system where the SVC installed in the system. It is to be noted that optimal values of PSSs and SVC parameters were used in the investigation. These values were also obtained using the method proposed in [7, 8] and are given in Table 5. There is a damping improvement for the inter-area mode when the SVC is installed (compare the damping ratio in Table 2 with Table 3). This results show that the SVC is able to provide better system stability.

Table 4 Electromechanical inter-area mode for system with PSSs and SVC

Eigenvalue	Frequency	Damping Ratio
-0.8908±j4.1701	0.66	0.2089

Tabel 5 PSSs parameters (system with PSSs and SVC)

Controller	Parameter	Value
PSS at G1	K_{PSS}	16.8082 pu
	T_{PSS}	1.0576 s
	T_{PSS1}	0.3944 s
	T_{PSS2}	0.2072 s
	T_{PSS3}	0.0182 s
	T_{PSS4}	0.0639 s
PSS at G2	K_{PSS}	10.1706 pu
	T_{PSS}	1.0077 s
	T_{PSS1}	0.9530 s
	T_{PSS2}	0.2178 s
	T_{PSS3}	0.0145 s
	T_{PSS4}	0.1479 s
SVC	K_S	2.2365 pu
	T_S	0.0984 s
	T_{S1}	0.1004 s
	T_{S2}	0.1217 s
SDC	K_{SDC}	0.5314 pu
	T_{SDC}	1.0367 s
	T_{SDC1}	0.1558 s
	T_{SDC2}	0.0258 s
	T_{SDC3}	0.1442 s
	T_{SDC4}	0.1609 s

4.3 Time-Domain Simulation

Although the results given in Section 4.2 have been confirmed by eigenvalue calculations, it is desirable to investigate the performance of the controllers in the time-domain under a large disturbance. The disturbance is a three-phase fault on a busbar section connected to node N8 via a bus coupler. The fault is initiated at time t = 0.10 second, and the fault clearing time is 0.05 second with the bus coupler tripping.

The improvement in performance is quantified by comparing the time-domain responses in Figures 6 - 8. As the critical mode is the inter-area mode, the responses used in the comparisons are those of the active-power flow transients in tie line connecting nodes N9 and N10.

From the responses, it can be seen that, without controllers (PSSs and/or FACTS device), the system oscillation is poorly damped and takes a considerable time to reach a stable condition (see Figure 6). Figure 7 shows the system transients with two PSSs installed in the system. There are some improvements in oscillation settling time with PSSs installed in the system (compare Figure 6 with Figure 7).

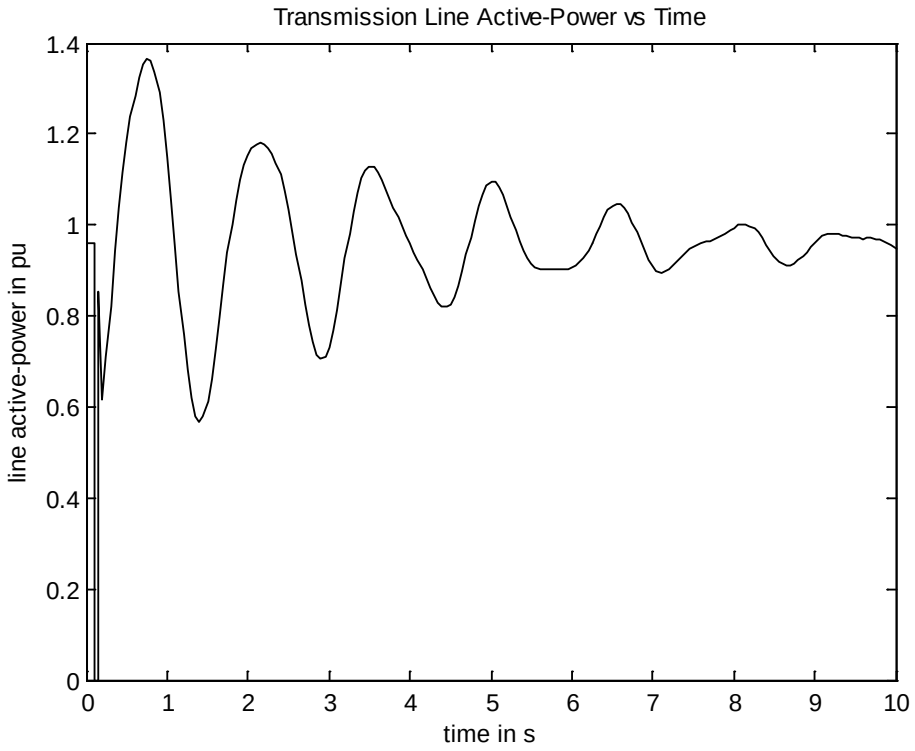

Figure 6 System transient (without PSSs and SVC)

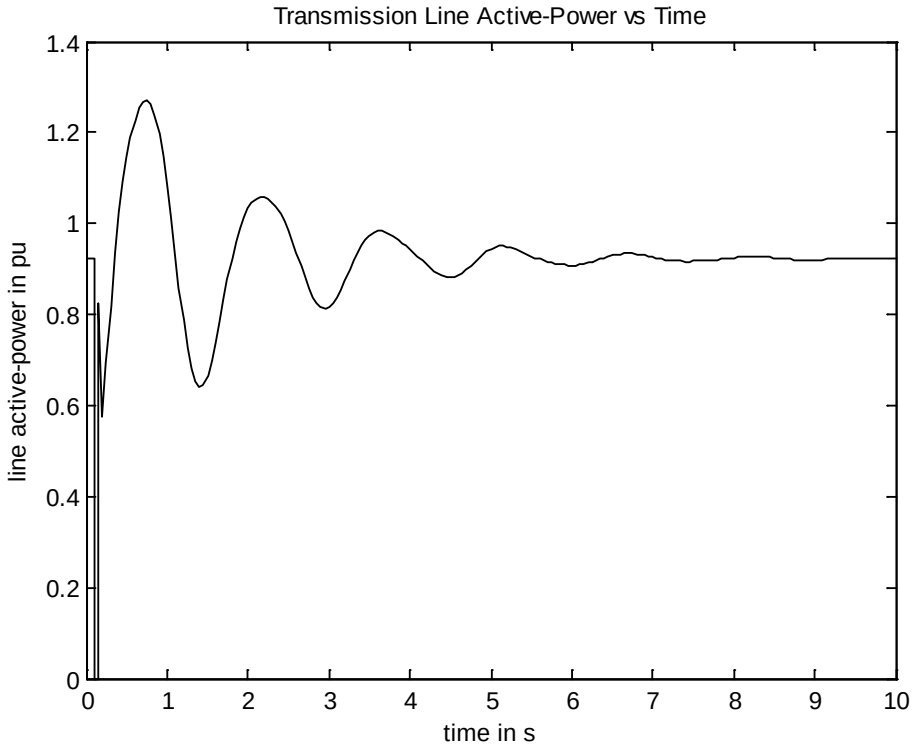

Figure 7 System transient (with PSSs)

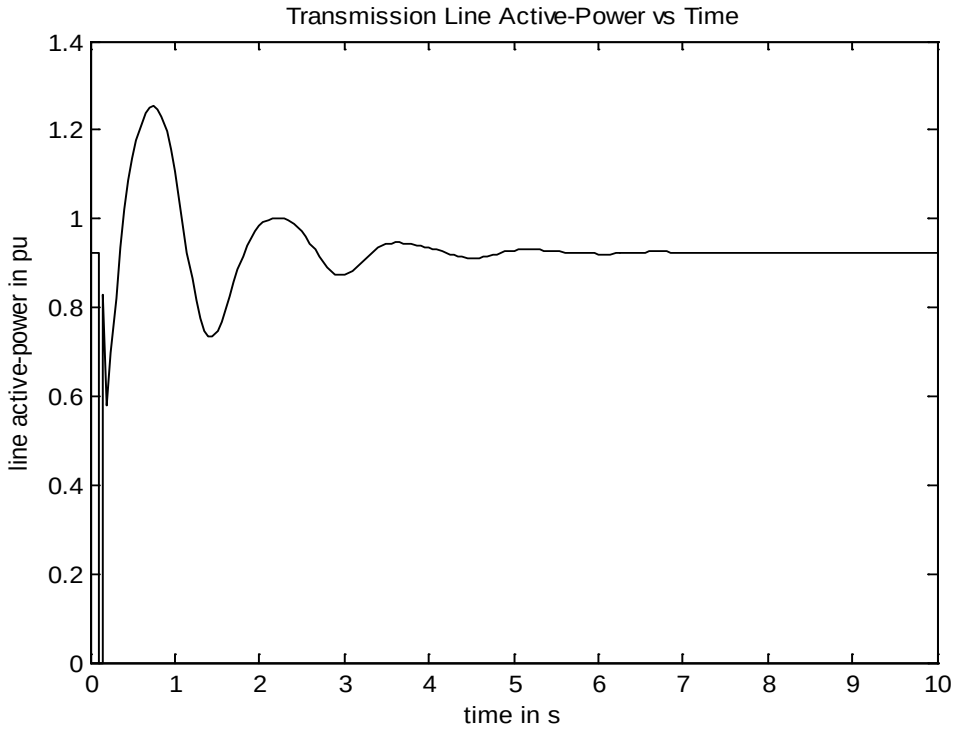

Figure 8 System transient (with PSSs and SVC)

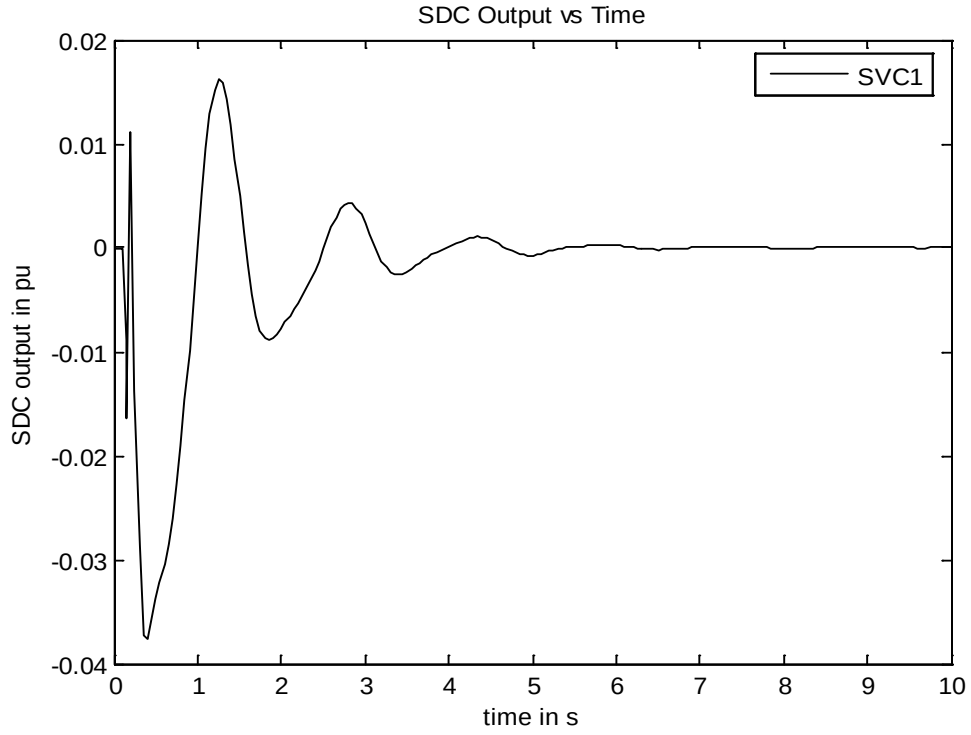

Figure 9 Transient of SVC's supplementary controller output

Further improvement in the inter-area oscillation settling time is obtained with the SVC and its supplementary controller installed in the system. The oscillation is damped more quickly as shown in Figure 8. Figure 8 confirms a good system dynamic performance when SVC and its supplementary controller are installed in the power system.

In Figure 9 is also shown in a graphical form the output of supplementary controller of SVC during the transient period following the disturbance. In the time-domain simulation, supplementary controller output limiter is represented. The supplementary controller output amplitude is limited to a band of 5%. Figure 9 shows further the confirmation of the SVC performance under large disturbance. It can be seen from Figure 9 that during a first few seconds of the transient period, the supplementary controller gives higher outputs, and therefore, provides significant contribution to the system damping and dynamic performance.

5 Conclusion

In this paper, the application of SVC in improving the system electromechanical oscillation damping and stability of an interconnected multi-machine electric power system has been investigated. The main contributions of the present paper can be described as follows: (i) development of general mathematical model of multi-SVC in multi--machine power system environment for stability studies. By using the mathematical formulation proposed, any number of SVCs (installed in any buses) can be modelled without difficulty. Also it can be applied to any size of power system; (ii) application and extension of the method for control coordination of PSSs and SVC to multi-machine power system, with a particular reference to the enhancement of inter-area mode damping. The performance of FACTS device (i.e. SVC) in improving system oscillation damping and stability is validated by eigenvalues analysis and time-domain simulations of the power system.

Appendix

A.1 Matrix Expressions of SVC Controllers

SVC main controller:

$$\boldsymbol{A}_S = \begin{bmatrix} -\frac{1}{T_S} & 0 \\ \frac{T_S - T_{S1}}{T_S T_{S2}} & -\frac{1}{T_{S2}} \end{bmatrix}$$

$$\boldsymbol{B}_S = \begin{bmatrix} -\frac{K_S}{T_S} \\ -\frac{K_S T_{S1}}{T_S T_{S2}} \end{bmatrix}$$

$$\boldsymbol{C}_S = \begin{bmatrix} -\frac{K_S}{T_S} \\ -\frac{K_S T_{S1}}{T_S T_{S2}} \end{bmatrix}$$

$$\boldsymbol{D}_S = \begin{bmatrix} \frac{K_S}{T_S} \\ \frac{K_S T_{S1}}{T_S T_{S2}} \end{bmatrix}$$

SVC supplemantary controller:

$$\boldsymbol{A}_{su} = \begin{pmatrix} -\frac{1}{T_{SDC1}} & 0 & 0 \\ \frac{T_{SDC} - T_{SDC1}}{T_{SDC} . T_{SDC2}} & -\frac{1}{T_{SDC2}} & 0 \\ \frac{T_{SDC3}}{T_{SDC4}}\left(\frac{T_{SDC} - T_{SDC1}}{T_{SDC} T_{SDC2}}\right) & \frac{T_{SDC2} - T_{SDC3}}{T_{SDC2} T_{SDC4}} & -\frac{1}{T_{SDC4}} \end{pmatrix}$$

$$\boldsymbol{C}_{su} = \begin{bmatrix} K_{SDC} \\ \frac{K_{SDC} T_{SDC1}}{T_{SDC2}} \\ \frac{K_{SDC} T_{SDC1} T_{SDC3}}{T_{SDC2} T_{SDC4}} \end{bmatrix}$$

A.2 System Data

Table A.1 Machine constants

	Gen. 1	Gen. 2	Gen. 3	Gen. 4
Ra	0.00028	0.00028	0.00028	0.00028
Xd	0.2	0.2	0.2	0.2
Xq	0.19	0.19	0.19	0.19
Xmd	0.178	0.178	0.178	0.178
Xmq	0.168	0.168	0.168	0.168
Xkd	0.50	0.50	0.50	0.50
Xkq	0.2218	0.2218	0.2218	0.2218
Xfd	0.1897	0.1897	0.1897	0.1897
Rkd	0.01	0.01	0.01	0.01
Rkq	0.001471	0.001471	0.001471	0.001471
Rfd	0.000063	0.000063	0.000063	0.000063
H	60	60	60	60

Table A.2 Transmission line data

Line	Node	Impedance	Shunt Admitance
1	N3 – N5	0.0010 + j0.0120	0
2	N2 – N6	0.0010 + j0.0120	0
3	N1 – N8	0.0010 + j0.0120	0
4	N4 – N7	0.0010 + j0.0120	0
5	N5 – N12	0.0025 + j0.0250	j0.150
6	N6 – N9	0.0010 + j0.0100	j0.030
7	N6 – N12	0.0013 + j0.0125	j0.075
8	N7 – N10	0.0010 + j0.0100	j0.030
9	N7 – N11	0.0013 + j0.0125	j0.075
10	N8 – N11	0.0013 + j0.0125	j0.075
11	N9 – N10	0.0074 + j0.0734	j0.990
12	N9 – N10	0.0074 + j0.0734	j0.990

References:

[1] S. Manoj and Puttaswamy P.S.: 'Importance of FACTS controllers in power systems', *International Journal of Advanced Engineering Technology*, 2011, Vol. 2, No. 3, pp. 207-212.

[2] Nguyen, T.T., and Gianto, R.: 'Application of optimization method for control co-ordination of PSSs and FACTS devices to enhance small-disturbance stability', *Proceedings of the IEEE PES 2005/2006 Transmission and Distribution Conference & Exposition*, May 2006, pp. 1478-1485.

[3] Singhal, P.: 'Advanced Adaptive Particle Swarm Optimization based SVC Controller for Power System Stability', *International Journal of Intelligent Systems and Applications*, 2015, Vol. 1, pp. 101-110.

[4] Ali, E.S., and Abd-Elazim, S.M.: Power System Stability Enhancement via New Coordinated Design of PSSs and SVC', *WSEAS Transactions on Power Systems*, 2014, Vol. 9, pp. 428-438.

[5] Bian, X.Y., et al.: 'Coordination of PSSs and SVC Damping Controller to Improve Probabilistic Small-Signal Stability of Power System with Wind Farm Integration', *IEEE Transactions on Power Systems*, 2016, Vol. 31, No. 3, pp. 2371-2382.

[6] Zuo, J., Li, Y., Shi, D., and Duan, X.: 'Simultaneous Robust Coordinated Damping Control of PSSs, SVC and DFIG PODs in Multimachine Power Systems', *Energies*, 2017, Vol. 10, pp. 1-23.

[7] Nguyen, T.T., and Gianto, R.: 'Stability improvement of electromechanical oscillations by control co-ordination of PSSs and FACTS devices in multi-machine systems', *Proceedings of the IEEE PES GM 2007*, June 2007, pp. 1-7.

[8] Nguyen, T.T., and Gianto, R.: 'Optimisation-based control co-ordination of PSSs and FACTS devices for optimal oscillations damping in multimachine power system', *IET Gener. Transm. Distrib.*, 2007, Vol. 1, No. 4, pp.564-573.

[9] CIGRE Working Group, Transmission Systems Committee: 'Modeling of static shunt var systems (SVS) for system analysis', *Electra*, October 1976, Vol. 51, pp. 45-74.

[10] CIGRE TF 38.01.08: 'Modeling of power electronics equipment (FACTS) in load flow and stability programs: a representation guide for power system planning and analysis', 1999.

[11] Padiyar, K.R.: *Power System Dynamics Stability and Control*, 1996, John Wiley & Sons (Asia) Pte Ltd, Singapore.

[12] Cai, L.J., and Erlich, I.: 'Simultaneous coordinated tuning of PSS and FACTS damping controllers in large power systems', *IEEE Trans. Power Systems*, 2005, Vol. 20, No. 1, pp. 294-300.

[13] Pourbeik, P., and Gibbard, M.J.: 'Simultaneous coordination of power system stabilizers and FACTS device stabilizers in a multimachine power system for enhancing dynamic performance', *IEEE Trans. Power Systems*, 1998, Vol. 13, No. 2, pp. 473-479.

[14] Pal, B.C., Coonick, A.H., Jaimoukha, I.M., and El-Zobaidi, H.: 'A linear matrix inequality approach to robust damping control design in power systems with superconducting magnetic energy storage device', *IEEE Trans. Power Systems*, 2000, Vol. 15, No. 1, pp. 356-362.

[15] Majumder, R., Chaudhuri, B., El-Zobaidi, H., Pal, B.C., and Jaimoukha, I.M.: 'LMI approach to normalised $\mathbf{H}_\infty$ loop-shaping design of power system damping controllers', *IEE Proc.-Gener. Transm. Distrib.*, 2005, Vol. 152, No. 6, pp. 952-960.